journal

J. Am. Ceram. Soc., 73 [6] 1674–80 (1990)

Fiber Debonding in Residually Stressed Brittle Matrix Composites

Panos G. Charalambides*,*

Materials Department, College of Engineering, University of California, Santa Barbara, California 93106

The competition between initial fiber debonding versus fiber failure marks a crucial event of the microstructural failure process in fiber-reinforced brittle matrix composites. In this study, the role of a thermal residual stress field on the debonding conditions is examined theoretically and analytically. The analysis is based on two critical observations, the first being that the mechanics at the tip of a kink crack are driven *only* by the *singularity* at the main crack tip. Following from the first is the second observation that any thermal stress effects on the debonding criteria should enter only through the phase angle ψ^T of the total stress intensity factor at the main crack tip. In general, this stress intensity factor has a thermal as well as a mechanical load contribution. It is shown that when the thermal and mechanical stress intensities, K^R and K', respectively, are *in phase*, i.e., $\psi^R = \psi'$, the existing debonding conditions are universal and can be used even in the presence of thermal loads. On the contrary, when K^R and K' are *out of phase*, i.e., $\psi^R \neq \psi'$, events such as the delamination of *thick* films or debonding of *inclined aligned fibers* in brittle matrix composites become sensitive to the presence of the thermal stresses. [Key words: composites, brittle materials, fibers, stress, debonding.]

I. Introduction

THE "ductility" and toughness of brittle matrix fiber-reinforced composite systems crucially depend on the competing effect of initial fiber debonding versus fiber failure.[1,2] The choice of the favored event is made at the microstructural level by the matrix crack early on in the failure process of the composite. Initiation of *matrix cracking* marks the first step of failure of the composite. The mechanics for this phenomenon have been extensively analyzed in recent years.[3–5] Subsequent to matrix cracking initiation, the matrix crack driven by the mode I[6] stress intensity factor, K_I, propagates through the matrix and intercepts the fiber reinforcements (Fig. 1(A)), an event that signifies the beginning of the second step of microstructural failure. At this configuration (Fig. 1(A)), the matrix crack, still dominated by the opening mode (mode I), eventually favors one of two virtual crack paths: the mode I straightforward path (Fig. 1(B)) or the mixed-mode[7–11] interface path (Fig. 1(C)). In the first case, if the available energy release rate at the 0° fiber kink crack (Fig. 1(B)) exceeds the fracture toughness of the fiber $\mathcal{G}_{fc}$, the matrix crack encounters no further resistance and thus propagates catastrophically through the fiber reinforcements triggering a *brittle type failure* of the composite, resulting in minimum or no macroscopic "ductility" and composite toughness. On the other hand, if the crack kinks at a 90° angle relative to the initial matrix crack plane, i.e., *fiber debonding* along the fiber matrix interface (Fig. 1(C)), substantial toughening can occur because of fiber bridging and/or subsequent frictional fiber pullout, as discussed elsewhere.[7,12–15] Thus, in optimally designed high-toughness fiber-reinforced systems, initial fiber debonding is a salient feature of the composite microstructural failure and marks the activation of various toughening processes in the composite. Despite its importance, rigorous solutions pertinent to initial fiber debonding conditions were unavailable until recently.

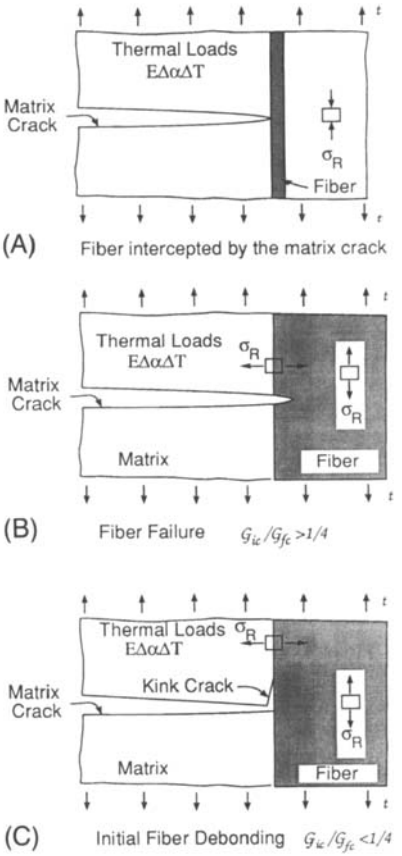

Fig. 1. Schematic of composite microstructural failure. (A) The fiber is intercepted by the matrix crack. (B) Fiber failure. For a homogeneous system, *fiber failure* will be favored over initial fiber debonding (Fig. 1(C)) if $\mathcal{G}_{ic}/\mathcal{G}_{if} > 1/4$, as discussed in Refs. 8–10. (C) Onset of initial fiber debonding. For a homogeneous system, if $\mathcal{G}_{ic}/\mathcal{G}_{if} \leq 1/4$ (Refs. 8–10) *initial fiber debonding* is favored over fiber failure (Fig. 1(B)).

D. Marshall—contributing editor

Manuscript No. 198232. Received July 21, 1989; approved December 11, 1989.

Supported by the Defense Advance Research Project Agency through the University Research Initiative at UCSB under Contract N-00014-86-K-0753.

*Member, American Ceramic Society.

*Current address: Department of Mechanical Engineering and Engineering Mechanics, Michigan Technological University, Houghton, MI 49931.

In characterizing the debonding process, He and Hutchinson,[9] Evans *et al.*[10] and Thouless *et al.*[11] derived conditions for fiber failure versus initial fiber debonding pertinent to the competing fracture processes depicted in Figs. 1(B) and (C), respectively. Such debonding conditions were obtained[9,10] for a wide range of bimaterial systems, interface characteristics, and fiber orientation. In their studies, He and Hutchinson[9] were concerned with two competing incipient kink cracks (cracks of infinitesimal length), i.e., the fiber and the debond kink cracks shown schematically in Figs. 1(B) and (C), respectively. To assure generality of their solutions, the energy release rates and the phase angles at the tip of each of these incipient cracks were obtained from an *existing* singular stress field at the tip of the main matrix crack and the corresponding kink angle relative to the matrix crack plane. Subsequently, fiber debonding conditions were derived from the ratio $\mathcal{G}^k/\mathcal{G}^T$, where $\mathcal{G}^k$ and $\mathcal{G}^T$ are the computed energy release rates at the tip of the interface (Fig. 1(C)) and fiber (Fig. 1(B)) kink cracks, respectively. In summary, for a homogeneous composite system and for a network of reinforcements aligned in the direction of the applied loads at 90° from the matrix crack plane (Fig. 1(A)), fiber debonding was found to be favored over fiber failure when $\mathcal{G}_{ic}/\mathcal{G}_{fc} \leq 1/4$ is satisfied, where $\mathcal{G}_{ic}$ and $\mathcal{G}_{fc}$ are the fracture toughnesses of the interface and the fiber, respectively. In this particular example, the matrix crack is dominated by a mode I stress intensity factor even in the presence of thermal loads. To the extent of the above assumptions, the existing criteria[8-11] for cracks kinking out of interfaces or cracks deflecting along weak interfacial paths are general and can be used to study fiber debonding in brittle matrix composite systems. However, recent discussions yielded an additional need to assess and clarify the role, if any, of a thermal residual stress field on fiber debonding.

Composite systems develop thermal residual stresses during processing because of thermal expansion mismatches between the fiber and the matrix. These stresses are known to substantially influence the mechanical properties and toughness in these composites. For example, Charalambides and Evans,[7] from a finite element analysis in composites with interfacial residual tension, found that the mechanics at the tip of a debond crack (kink crack of finite length) sensitively depend on the thermal stresses. In light of this, a fundamental question is put forward. The findings of He and Hutchinson are for a kink crack of infinitesimal length: Can these results be used to predict fiber debonding conditions in the presence of appreciable thermal residual stresses?

In this work, a theoretical argument and analytical considerations in the case of a homogeneous system are employed to clarify the stated question. The analysis employed in this study is general and applies to systems with main cracks under *out-of-phase* complex stress intensities caused separately by the thermal and mechanical loads. Special cases of practical interest are presented as examples, such as fiber debonding in unidirectionally fiber-reinforced composite systems and delamination of thick films subjected to both mechanical and thermal stresses. Furthermore, some of the issues presented in this analysis are similar to those encountered in the analysis for continuing fiber debonding versus fiber failure at the tip of a finite debond crack, an equally important step in completing our understanding of the microstructural failure process in brittle matrix composites. This phenomenon is taken on in the discussion section of the present study.

II. Debonding Mechanics

For the sake of the analysis, let us consider the cylindrical unit cell shown in Fig. 2. This configuration corresponds to a fully cracked matrix while the crack is bridged by the intact fiber reinforcements. The stresses and strains in the crack tip region (homogeneous system) are dominated by the singular-

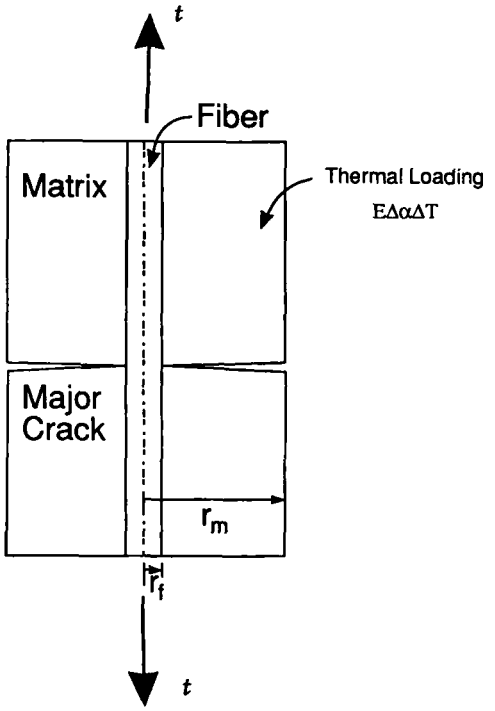

Fig. 2. Axisymmetric cylindrical unit cell wherein the matrix crack is bridged by an aligned network of fiber reinforcements.

ity of the main matrix crack. Because of the symmetry of the unit cell and for both the applied and thermal load cases, the matrix crack is constrained to a symmetrical relative crack surface opening such that only K_I, the mode I stress intensity factor is nonzero. These observations essentially determine the mechanics of fiber debonding. In particular, the competing effects of initial fiber debonding versus fiber failure can be examined by comparing the energy release rate $\mathcal{G}^k$ at the tip of the kink crack (kink angle 90°), to that of the main crack $\mathcal{G}^T$ due to the combined effects of applied and thermal loadings. However, as discussed by Cotterell and Rice,[16] the stress intensity factors at the tip of an infinitesimal kink crack depend only on the original *singular* stresses at the main crack tip. Any nonsingular stress terms, including thermal stresses and contacting asperity tractions, cancel out or, if introduced on the kink crack surfaces, will give zero contribution to the kink crack stress intensities and energy release rate. Moreover, as indicated above, both the applied and thermal loads give rise only to a mode I stress intensity factor. Thus, the stress intensities at both kinds of kink cracks are proportional to the main crack K_I, and the ratio $\mathcal{G}^k/\mathcal{G}^T$ is that which would be produced by mechanical loading alone. It follows that under these assumptions, the conditions derived by He and Hutchinson,[8,9] Evans *et al.*,[10] and Thouless *et al.*[11] can be used to predict which of the critical events would occur first even in the presence of thermal loads. However, there is an additional interest in cases wherein the assumption is violated that the mechanical and thermal loads produce only mode I matrix crack stress intensities. Such conditions for instance prevail during delamination of thermally bonded *thick* films and possibly during debonding of *inclined aligned* fiber reinforcements. For these systems, a more rigorous analysis is needed to clarify the thermal effects on initial debonding/delamination conditions. Such analysis, based on near-tip mechanics, is presented below.

(1) Cracks Kinking out of a Mixed-Mode Crack Tip

In this section the analysis is extended to include the thermal effects on debonding or crack kinking at the tip of a mixed-mode crack. To be more specific, consider a situation

in which an applied load t and a thermal load σ^R, with $\sigma^R = E\Delta\alpha\Delta T$ being a residual stress measure, are imposd on the composite. There are then two contributions to the complex stress intensity factor K^T at the main matrix crack tip (Fig. 3): (i) K^t due to the applied loads t and (ii) K^R being the contribution of the thermal loads σ^R. From existing solutions[6,7] and dimensional analysis, the above stress intensities can be written in a complex form as

$$K^t = K_I^t + iK_{II}^t = ta^{1/2}F^t(\cos\psi^t + i\sin\psi^t) \quad (1a)$$

$$K^R = K_I^R + iK_{II}^R = \sigma^R a^{1/2}F^R(\cos\psi^R + i\sin\psi^R) \quad (1b)$$

where F^t and F^R are, in the general case of a bimaterial system, nondimensional functions of geometry and bimaterial elastic properties.[6,7] Then, the combined total complex stress intensity factor K^T at the tip of the main crack is obtained via linear superposition as follows:

$$K^T = K_I^T + iK_{II}^T = \left(1 + \frac{K_I^R}{K_I^t}\right)K_I^t + i\left(1 + \frac{K_{II}^R}{K_{II}^t}\right)K_{II}^t \quad (2)$$

The total energy release rate at the matrix crack tip is obtained in terms of $|K^T|$, the modulus of K^T, via Irwin's relationship for cracks in homogeneous bodies, i.e.

$$\mathcal{G}^T = \frac{1-\nu^2}{E}[(K_I^T)^2 + (K_{II}^T)^2]$$

$$= \frac{1-\nu^2}{E}(K_I^T)^2(1 + \tan^2\psi^T) \quad (3)$$

with E being the Young's modulus and ν the Poisson's ratio of the material. Following Cotterell and Rice,[16] the combined stress intensity factor at the tip of the kink crack has two components, K_1^k and K_2^k, and can be obtained from K^T, the total stress intensity factor at the tip of the main crack, as follows:

$$K_1^k = c_{11}K_I^T + c_{12}K_{II}^T \quad (4a)$$

$$K_2^k = c_{21}K_I^T + c_{22}K_{II}^T \quad (4b)$$

where c_{ij} $(i, j = 1, 2)$ are geometric factors which for a homogeneous system are given in terms of the kink angle θ (Fig. 3) and coincide with Cotterell and Rice values[16] for low values of θ. From Irwin's relationship and in light of the above equations, the total energy release rate at the kink crack $\mathcal{G}^k$ becomes

$$\mathcal{G}^k = \frac{1-\nu^2}{E}[(K_1^k)^2 + (K_2^k)^2]$$

$$= \frac{1-\nu^2}{E}(K_I^T)^2 C(c_{ij}(\theta),\psi^T) \quad (5)$$

where

$$C(c_{ij}(\theta),\psi^T) = c_{11}^2 + c_{21}^2 + 2(c_{11}c_{12} + c_{21}c_{22})\tan\psi^T + (c_{12}^2 + c_{22}^2)\tan^2\psi^T \quad (6)$$

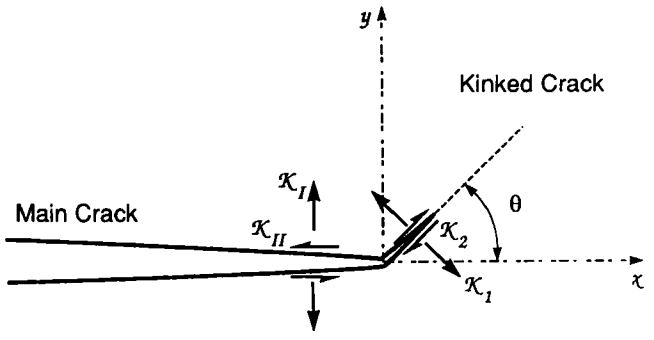

Fig. 3. Schematic of a main crack kinking under mixed-mode conditions.

and $\tan\psi^T = K_{II}^T/K_I^T$ is the phase angle for the total stress intensity factor at the tip of the matrix crack and is obtained from Eq. (2) as follows:

$$\tan\psi^T = \frac{K_{II}^T}{K_I^T} = \frac{1 + \dfrac{F^R}{F^t}\dfrac{\sin\psi^R}{\sin\psi^t}\dfrac{\sigma^R}{t}}{1 + \dfrac{F^R}{F^t}\dfrac{\cos\psi^R}{\cos\psi^t}\dfrac{\sigma^R}{t}}\tan\psi^t \quad (7)$$

(2) Debonding Conditions

The competing effects of crack kinking (fiber debonding, Fig. 1(C)) versus fiber failure (Fig. 1(B)) can be established using Eqs. (3) and (5) to obtain a condition for the toughness ratio $\mathcal{G}_{ic}/\mathcal{G}_{fc}$, which is the fracture toughness of the interface to the fracture toughness of the fiber. Such an analysis is based on the implicit assumption that the system is ideally brittle and that fracture at the tip of the competing kink cracks is driven by the energy release rate alone. Also implicit in the analysis is the assumption that any possible increases in $\mathcal{G}_{ic}$ due to the increased mode mixity ψ^k at the kink crack tip ($\psi^k \approx 42°$, Ref. 9) are neglected. However, as discussed by Evans and Hutchinson,[17] nonunique values for $\mathcal{G}_{ic}$ are obtained at nonzero phase angles $\psi \neq 0$. The increase in $\mathcal{G}_{ic}$ with ψ is primarily due to contacting asperities on the crack surfaces behind the crack tip, as discussed elsewhere.[17] In the case of an incipient kink crack, i.e., a kink crack of infinitesimal length, such effects are minimal and therefore an energy release rate criterion can be used to predict kink crack initiation, as implemented by He and Hutchinson,[8,9] Evans *et al.*,[10] and Thouless *et al.*[11] Thus, in the absence of any shielding effects at the kink crack tip due to contacting asperities and in an ideally brittle environment, fracture occurs when $\mathcal{G}^k \geq \mathcal{G}_{ic}(\psi^k = 0°)$ with $\mathcal{G}_{ic}(\psi^k = 0°)$ being the mode I fracture toughness of the interface. In particular when the competition is between a kink crack at 90° from the plane of the main crack (Fig. 1(C)) and fiber failure (Fig. 1(B)), fiber debonding is favored when

$$\frac{\mathcal{G}_{ic}}{\mathcal{G}_{fc}} \leq [c_{11}^2 + c_{21}^2 + 2(c_{11}c_{12} + c_{21}c_{22})\tan\psi^T + (c_{12}^2 + c_{22}^2)\tan^2\psi^T]_{\theta=\pi/2}/(1 + \tan^2\psi^T) \quad (8)$$

On the other hand, if kinking occurs at an angle other than 90° with respect to the plane of the main crack such as the case of debonding along the interface of inclined fibers (Fig. 4), the favored event is obtained by comparing the solutions for the energy release rate at the tip of two competing inclined kink cracks, as shown in Figs. 4(B) and (C). In this instance, fiber debonding is favored over a fiber failure if

$$\frac{\mathcal{G}_{ic}}{\mathcal{G}_{fc}} \leq [c_{11}^2 + c_{21}^2 + 2(c_{11}c_{12} + c_{21}c_{22})\tan\psi^T + (c_{11}^2 + c_{21}^2)\tan^2\psi^T]_{\theta=\theta_i}/[c_{11}^2 + c_{21}^2 + 2(c_{11}c_{12} + c_{21}c_{22})\tan\psi^T + (c_{12}^2 + c_{22}^2)\tan^2\psi^T]_{\theta=\theta_f} \quad (9)$$

where θ_i and θ_f are the kink angles for the debond and fiber kink cracks, and are shown schematically in Figs. 4(B) and (C), respectively. It becomes clear from Eqs. (8) and (9) that the thermal loads influence the debonding condition via the phase angle ψ^T *only*, which is given by Eq. (7). To be more specific, when $\psi^R = \psi^t$, i.e., *in-phase* thermal-mechanical stress intensities, Eq. (7) yields that $\psi^T = \psi^t$ and the thermal effects do not enter the conditions given by Eqs. (8) and (9). On the contrary, when $\psi^R \neq \psi^t$ the above conditions become sensitive to the thermal loads via Eq. (7), in which case additional analysis is needed in order to clarify the thermal effects.

To further explore and quantify each of the above possibilities, studies pertinent to debonding in homogeneous sys-

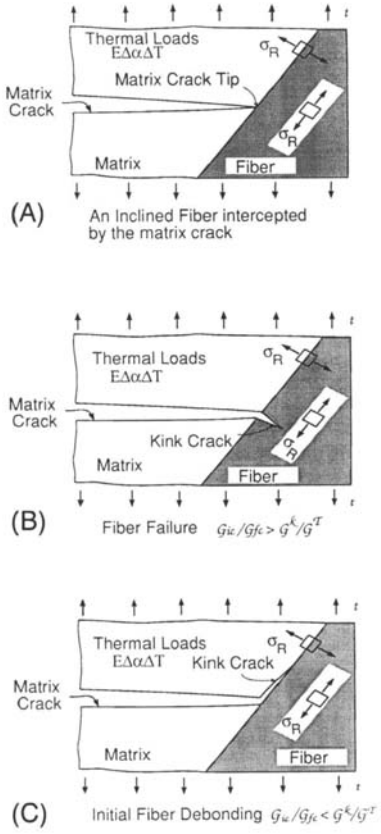

Fig. 4. Schematic of competing events of debonding versus fiber failure for systems with interfaces inclined relative to the matrix crack plane.

tems with interfaces are presented below for two special cases. Initially, we consider the case in which the thermal and mechanical loads when applied independently give rise to *in-phase* stress intensities at the tip of the main crack so that $\psi^T = \psi' = \psi^R$ and the thermal effects drop out of the debonding conditions. Subsequently, we consider the case in which the thermal and mechanical stress intensities are *out of phase*, i.e., $\psi^R \neq \psi'$, and debonding does depend on the thermal loads.

III. Debonding Independent of Thermal Loads

In the case where the mechanical and thermal loads independently give rise to *in-phase* stress intensities at the main crack tip, i.e., $\psi' = \psi^R$, Eq. (7) yields $\psi^T = \psi' = \psi^R$. As a result, the debonding conditions expressed via Eqs. (8) and (9) become *independent* of the thermal loads and can be determined from the mechanical loads alone. Some of the conditions derived by He and Hutchinson and Evans *et al.* implicitly assumed in-phase mode I thermal and mechanical stress intensities and are universal to the extent of the above assumption. To demonstrate the validity of those results, we shall now consider the fiber debonding processes for the composite unit cell shown in Fig. 2. As discussed earlier in this work, the matrix crack (Fig. 2) is dominated by a mode I stress intensity factor due to either mechanical or thermal loading and thus $\psi^T = \psi^R = \psi' = 0$. These conditions prevail at the tip of matrix cracks in systems such as fiber-reinforced composites with the network of fiber reinforcements aligned in the direction of the applied stress at 90° relative to the matrix crack plane (Fig. 1) or composite systems reinforced by a randomly oriented network of chopped fibers (Fig. 4), where on the average the thermal shear stress goes to zero. Also similar mode I conditions due to thermal and applied loads exist at the tip of the notch in the plane strain mode I prenotched bimaterial beam shown in Fig. 5. Therefore, in these systems and in light of Eq. (8), fiber debonding or onset of delamination of the top layer (Fig. 5) will be favored if

$$\frac{\mathcal{G}_{ic}}{\mathcal{G}_{fc}} \leq [c_{11}^2 + c_{21}^2]_{\theta=\pi/2} \tag{10}$$

which is a universal constant independent of thermal stresses. Furthermore, by using the approximate values for c_{11} and c_{21} obtained by Cotterell and Rice[16] in the case of a homogeneous system and for a kink angle $\theta = 90°$, the condition for fiber debonding given by Eq. (10) takes the form, $\mathcal{G}_{ic}/\mathcal{G}_{fc} \leq 1/4$, which is an approximate result first reported by Thouless *et al.*[11]

More exact results on fiber debonding conditions were recently obtained by He and Hutchinson[9] and Evans, He, and Hutchinson.[10] According to their findings, in a homogeneous system, fiber debonding is favored over fiber failure if $\mathcal{G}_{ic}/\mathcal{G}_{fc} \leq 1/5$. By comparison, it is clear that the debonding conditions given by Eqs. (8), (9), and (10) are quantitatively in slight error when the Cotterell and Rice[16] geometric factors $c_{ij}(\theta)$ are used, especially at large kink angles θ. However, the objective of this work is not to quantify the conditions for fiber debonding, but rather to qualitatively examine the effects of thermal loads on the fiber debonding condition. In that respect, the formulation presented in this work is general, provided that the decomposition of the stress intensity factor at the tip of the kink crack given via Eqs. (4) is valid. On the other hand, it can easily be shown that Eqs. (4) are derived via the principle of linear superposition, which is a characteristic property of any linear system. Therefore, the representation of the stress intensity factor at the tip of the kink crack via Eqs. (4) is general and is always valid in linear systems. Thus, it follows that the analysis presented in this article is general and can be extended to include bimaterial cases. For the latter case, the coefficients c_{ij} should properly be adjusted to account for elastic mismatches between the fiber and the matrix.

IV. Debonding Dependent on Thermal Loads

In the general case when the stress intensity factor at the main crack tip due to the thermal loads is out of phase with that due to the mechanical loads, i.e., $\psi^R \neq \psi'$, the debonding conditions (Eqs. (8) and (9)) are indeed sensitive to the presence of the thermal stresses via Eq. (7). To demonstrate the thermal effects on the above conditions we shall consider the example of the plane strain prenotched delamination four-point flexure specimen shown in Fig. 5. Without loss of generality, let us assume that the system is elastically homogeneous, i.e., $E_1 = E_2$ and $\nu_1 = \nu_2$, with E and ν being the Young's modulus and the Poisson's ratio, respectively, and the subscripts 1 and 2 denoting quantities for the top and bottom layers, respectively (Fig. 5). For the sake of the analysis let us

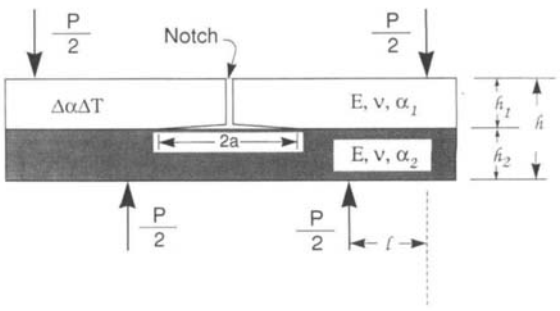

Fig. 5. Four-point delamination flexure specimen. The delamination process is competing against incipient kink cracks at the delamination crack tip.

also assume that the two thermally bonded layers have different thermal expansion coefficients, i.e., α_1 and α_2. Under these conditions and for the special case of a specimen with layers of *equal thickness*, $h_1 = h_2$, analytical solutions exist for the steady-state delamination mechanics[18-20] due to the applied and thermal loads. In particular, Charalambides *et al.*[18] and Suo and Hutchinson[19] found that the mechanical complex stress intensity factor due to the applied loads P is given by

$$K^t = \frac{1}{4}\left(\frac{2}{\sqrt{3}} + i\right) t h_2^{1/2} = t h_2^{1/2} \sqrt{\frac{7}{48}} e^{i(0.4089/1.8)\pi} \tag{11}$$

where $t = 3P\ell/bh_2^2$ is the maximum normal stress due to bending of the bottom layer alone. Thus, in this example the mechanical loads are characterized by a phase angle ψ^t such that $\tan \psi^t = \sqrt{3}/2$ or $\psi^t = 0.4089\pi/1.8$(rad) which is to a good approximation equal to 40.89°. In addition, the corresponding stress intensity factor due to the thermal loading $\sigma^R = E(\alpha_2 - \alpha_1)\Delta T$ was found by Charalambides *et al.*[20] to be a pure mode II and is given below:

$$K^R = i\frac{1}{4}\sigma^R h_2^{1/2} = \frac{1}{4}\sigma^R h_2^{1/2} e^{i(\pi/2)} \tag{12}$$

The thermal phase angle is $\psi^R = \pi/2$ and thus the thermal and mechanical loads give rise to *out-of-phase*, i.e., $\psi^R \neq \psi^t$, stress intensities at the delamination crack tip. In light of Eqs. (11) and (12), the expression for the phase angle of the total stress intensity factor ψ^T obtained from Eq. (7) reduces to

$$\tan \psi^T = \frac{\sqrt{3}}{2}(1 + \tau) \tag{13}$$

with $\tau = \sigma^R/t$. Further progress is made in the analysis by adopting for $c_{i,j}$ $(i, j = 1, 2)$ the approximate expressions derived by Cotterell and Rice.[16] Following Charalambides and Evans[7] and with the aid of Eq. (8), fracture at the tip of an incipient kink crack inclined at an angle β from the delamination crack plane (Fig. 3) is favored over further delamination when†

$$\frac{\mathcal{G}_{fc}}{\mathcal{G}_{ic}} \leq \frac{a_1(\beta) + a_2(\beta)\tan \psi^T + a_3(\beta)\tan^2 \psi^T}{1 + \tan^2 \psi^T} \tag{14}$$

with

$$a_1(\theta) = c_{11}^2 + c_{21}^2 = \frac{1}{8} + \frac{1}{2}\cos^2\frac{\theta}{2} + \frac{1}{4}\cos\theta + \frac{1}{8}\cos 2\theta$$

$$a_2(\theta) = 2(c_{11}c_{12} + c_{21}c_{22}) = -\sin\theta - \frac{1}{2}\sin 2\theta$$

$$a_3(\theta) = c_{12}^2 + c_{22}^2 = \frac{5}{8} + \frac{1}{2}\sin^2\frac{\theta}{2} + \frac{3}{4}\cos\theta - \frac{3}{8}\cos 2\theta \tag{15}$$

and β is the value for the kink angle θ for which $\mathcal{G}^k(\theta)$ given by Eqs. (5) and (15) becomes maximum. That is to say, from all virtual kink cracks the one with the maximum energy release rate is activated. This is usually assumed in the case of cracks kinking out of an interface[8] (Fig. 5). Thus, the situation considered here is somewhat different from those considered in the previous sections in this study. In those cases, e.g., fiber debonding, the angle β was fixed and taken to be equal to the interface orientation angle relative to the matrix crack plane (Fig. 1). On the contrary, the crack deflection angle in this analysis is unknown and is obtained as a part of the solution through an energy maximizing process. The maximum in $\mathcal{G}^k$ is obtained by first combining Eqs. (5) and (15) and then differentiating with respect to θ such that

$$\frac{d\mathcal{G}^k}{d\beta} = 0 \Rightarrow \frac{da_1}{d\beta} + \frac{da_2}{d\beta}\tan\psi^T + \frac{da_3}{d\beta}\tan^2\psi^T = 0 \tag{16}$$

where

$$\frac{da_1}{d\beta} = -\frac{1}{2}\sin\beta(1 + \cos\beta)$$

$$\frac{da_2}{d\beta} = 1 - \cos\beta(1 + 2\cos\beta)$$

$$\frac{da_3}{d\beta} = -\frac{1}{2}\sin\beta(1 - 3\cos\beta) \tag{17}$$

The trends for the total phase angle ψ^T and the kink angle β with the thermal-to-mechanical stress ratio σ^R/t for which a maximum in $\mathcal{G}^k$ is observed are shown in Fig. 6 in dashed and solid lines, respectively. The corresponding trend in the ratio $\mathcal{G}^T/\mathcal{G}^k$ is plotted on Fig. 7. It is of interest to observe some limiting cases. For example, as shown in Fig. 6 the phase angle of the total stress intensity factor ψ^T becomes negative for $\tau < -1.0$, which is consistent with Eq. (13). When the stress ratio $\tau = -1.0$, the total phase angle takes the value $\psi^T = 0$, in which case the delamination crack is dominated by only the mode I component of the applied stress intensity factor given by Eq. 10. In this instance, the maximum kink energy release rate occurs straight ahead of the delamination crack, i.e., $\beta = 0$ (Fig. 6), and the energy release rate ratio takes the value $\mathcal{G}^T/\mathcal{G}^k = 1.0$. Thus under ideally brittle conditions and when $\tau = -1.0$, the only favored fracture event is the failure of the interface under the influence only of the mode I component of the applied stress intensity factor. On the other hand, as the ratio $\tau = \sigma^R/t$ increases, failure of the bottom layer is favored over further delamination, as indicated by the failure map in Fig. 7. As shown in this figure, the competition between further delamination and failure in one of the two layers is most sensitive to the thermal stresses for small values of τ, i.e., $-2.0 \leq \tau \leq 2.0$. Outside this interval, the thermal effects become minimal.

V. Discussion

In this work, the effects of thermal stresses on the conditions for fiber debonding in brittle matrix composites and on the delamination criteria for thermally bonded plane strain layers have been examined. The analysis assumed elastically homogeneous systems but can be extended to include bimaterial

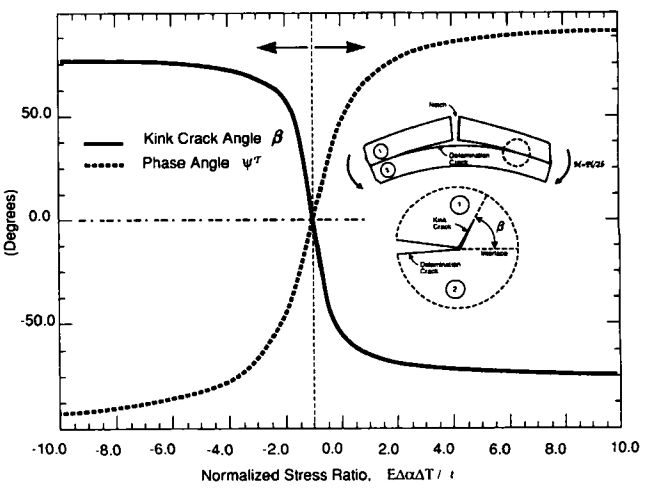

Fig. 6. Trends in the steady-state phase angle ψ^T (dashed line) and kinking angle β for which $\mathcal{G}^K$ is maximized (solid line) with the stress ratio σ^R/t, for the special case of a beam with $h_1 = h_2$.

†Eq. (14) in this article is identical to Eq. (12) in Ref. 7, where tan was erroneously replaced by arctan.

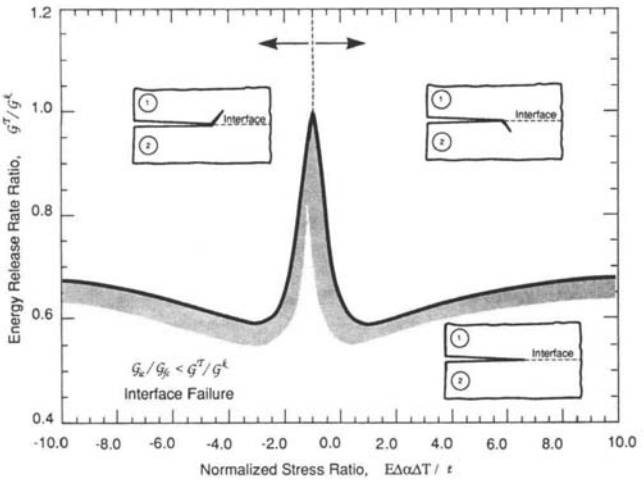

Fig. 7. *Trends in the ratio $\mathcal{G}^k/\mathcal{G}^T$ with the stress ratio σ^R/t in an otherwise elastically homogeneous system with thermal expansion mismatches between the top and bottom layers ($h_1 = h_2$).*

cases. Departing from the observation that the mechanics of incipient kink cracks are driven only by the singular stresses at the main crack tip, two distinct situations were examined in regard to the thermal effects on the debonding criteria. The first is the case when the thermal and mechanical loads give rise to *in-phase* stress intensities, i.e., $\psi^R = \psi'$, in which case the criteria for crack kinking are independent of the thermal loads. On the contrary, when the stress intensities are *out of phase,* i.e., $\psi^R \neq \psi'$, the criteria for delamination of thermally bonded layers and in some special cases the conditions for fiber debonding in brittle matrix composites, become sensitive to the presence of the thermal stresses.

In general, in fiber-reinforced brittle matrix composites, matrix cracking is a mode I process and remains as such even in the presence of thermal stresses. Thus, the existing[8-10] debonding criteria derived from a mode I matrix crack singularity can be used even in the presence of thermal loads. For example, earlier in this work, it was demonstrated that systems reinforced with an aligned fiber network oriented at 90° from the crack plane (Fig. 1) experience an in-phase mode I stress intensity at the matrix crack tip due to independent application of the applied and thermal loads. Thus, the condition for debonding reduces to Eq. (10) which is indeed independent of the thermal loads.

By analogy, the same conclusion must apply to systems reinforced with randomly oriented chopped fibers. Again in those systems, because of the randomness of the fiber orientation, a mode I stress intensity is induced at the matrix crack tip by both the thermal and applied loads. Thus, the debonding condition remains unaffected by the presence of thermal loads even if the fiber is intercepted at an angle by the matrix crack. Results for such systems are reported in the article by Evans, He, and Hutchinson.[10]

Unlike the previous two cases, a somewhat more complex situation is encountered in systems where the fiber reinforcements are both inclined and aligned relative to the matrix crack. For example, consider the near-tip schematic shown in Fig. 8. If the composite system is brittle, such that fiber failure (Fig. 8(A)) at the matrix crack surface is favored over fiber debonding (Fig. 8(B)), the stress intensity at the mechanically mode I matrix crack tip must remain mode I even in the presence of thermal loads. This is especially true for long matrix cracks (cracks extending over a substantial number of fibers), where the average thermal shear traction acting on the crack surfaces over the total crack length must be zero. As a result, a fiber failure criterion independent of thermal stresses must be obtained. On the other hand, when fiber debonding occurs prior to fiber failure (Fig. 8(B)), the inclined fibers would bridge the crack over a certain distance

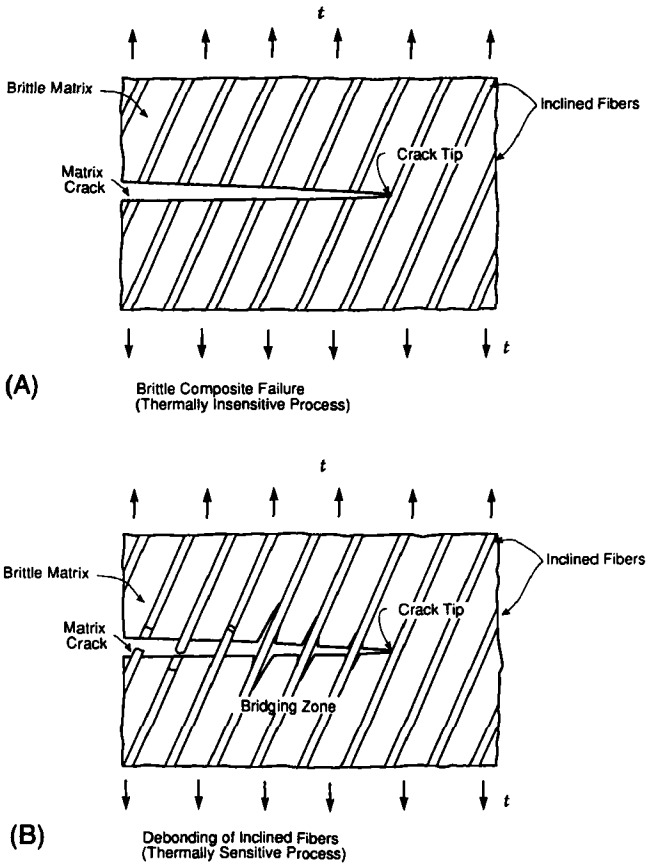

Fig. 8. *Schematics of the microstructural failure brittle matrix composites reinforced with an aligned and inclined fiber network. (A) Fibers failing without debonding. Low-toughness system.* (B) Fibers failing after debonding. High-toughness system.

from the matrix crack tip, as shown schematically in Fig. 8(B). Furthermore, debonding of inclined fibers is most likely geometrically asymmetric, and thus a mode II thermal component at the otherwise mode I matrix crack tip may exist. Under these conditions, fiber debonding would be influenced by the presence of thermal stresses. However, further studies are needed to clarify this case.

Finally, an example of thermally dependent kinking/delamination conditions was presented, via the equal thickness, elastically homogeneous four-point flexure beam specimen shown in Fig. 5. The delamination process is primarily mixed mode[18-21] and, in cases other than the thin-film decohesion process,[21] the thermal and mechanical stress intensities are not in phase. Thus, the delamination process in such systems must indeed depend on the thermal stresses as demonstrated earlier in this work, and fracture maps similar to that shown in Fig. 7 are needed to study these phenomena.

In light of the above observations, we now proceed to examine the processes of initial fiber debonding and further debond extension (delamination) in fiber-reinforced brittle matrix composites. In doing so, we employ the aid of Fig. 9 where the phase angles at the debond tip due to the applied load t and thermal load σ^R are plotted as a function of the debond crack length. The curve for ψ', the phase angle due to the applied loads, was obtained numerically by Charalambides and Evans[7] using finite elements. The curve for ψ^R (the thermal phase angle) is representative of composite systems stressed residually with their interfaces in tension and is qualitatively correct in the sense that only the steady-state result is reported in the literature.[7] Thus, knowing the steady-state result[7] together with the kink crack solution,[9] i.e., $(\psi^R)_{a=0} \approx 42.2°$, the transient branch for ψ^R is plotted qualitatively as shown in Fig. 9. However, the shape of this part of the curve is of no significance to the present analysis.

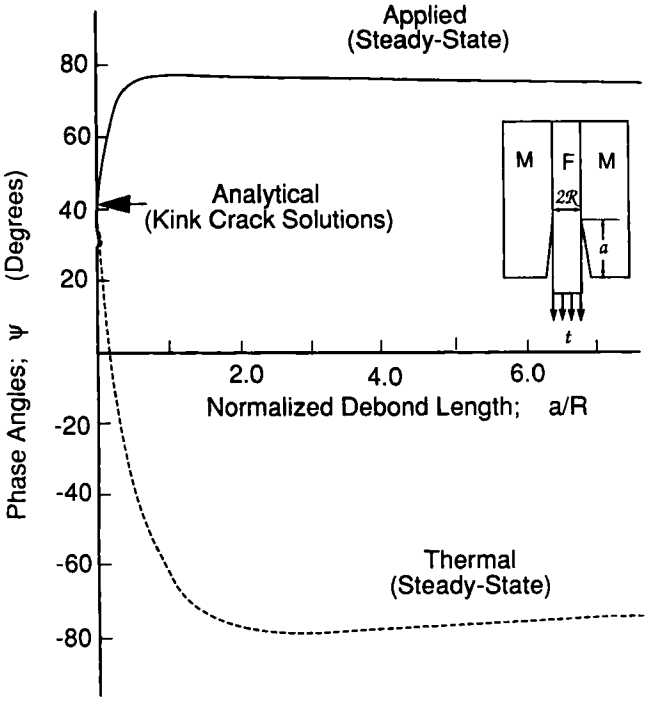

Fig. 9. Trends in the debond tip phase angles in a homogeneous system with normalized crack length. The curve for ψ' marked by the solid line was derived numerically (Ref. 7) via the method of finite elements for the case of an applied stress t alone. The dashed curve due to the thermal loads σ^R was interpolated between the steady-state numerical value reported in Ref. 7 and the kink crack solution derived in Ref. 9.

As shown in Fig. 9, at the limit $a \to 0$, the phase angles at the 90° debond kink crack due to the thermal and applied loads are equal, i.e., $\psi^R = \psi'$. This is obtained because of the dominance of the mode I singularity at the main matrix crack tip. Thus, using this result and by the virtue of earlier observations, initial debonding is insensitive to the presence of thermal stresses, and the criteria for this process to occur are given by He and Hutchinson[9] and Evans *et al.*[10] On the contrary, as the debond crack grows and enters the steady-state regime, i.e., $a \geq 5.0R$,[7] the thermal and applied debond-tip stress intensities are out of phase (Fig. 9), and the delamination process (debond extension) becomes indeed sensitive to the thermal stresses as discussed elsewhere.[7]

VI. Concluding Remarks

The effects of a thermal residual stress field on the condition for kink crack initiation relevant to fiber debonding in brittle matrix composite systems and on the delamination of layers in plane strain have been addressed. The analysis in this work is based on two critical observations. The singular stresses alone at the main crack tip drive the mechanics at the tip of all virtual kink cracks associated with that main crack tip. Given the above, any thermal effects on the kinking (fiber debonding/delamination) conditions enter via the phase angle ψ^T of the total stress intensity at the main crack the tip of all virtual kink cracks associated with that main crack tip. Given the above, any thermal effects on the kinking (fiber debonding/delamination) conditions enter via the phase angle ψ^T of the total stress intensity at the main crack tip. In particular, when ψ^T is independent of the thermal loads, i.e., $\psi^R = \psi'$, the conditions for debonding are also independent and the existing criteria for fiber debonding can be used even in the presence of thermal stresses. However, when $\psi^R \neq \psi'$, the coupled phase angle ψ^T does depend on the thermal stresses and the criteria for crack kinking versus further delamination or debond extension are thermally sensitive. Thus, such competing effects can be studied only using fracture maps involving the thermal stresses as well as the relative fracture toughnesses in the directions of the competing fracture events.

Acknowledgments: This analysis was precipitated by discussions with R. Cannon and L. Anderson at the 91st Annual Meeting and Exposition of the American Ceramic Society, Indianapolis, Indiana, April 1989. Discussions with R. M. McMeeking, A. G. Evans, and P. A. Mataga are gratefully acknowledged.

References

[1]A. G. Evans, "New High Toughness Ceramics"; in The Processing and Mechanical Properties of High Temperature/High Performance Composites. Annual Report, Department of Materials, University of California, Santa Barbara, CA, 1988.

[2]A. G. Evans, "The Mechanical Performance of Fiber Reinforced Ceramic Matrix Composites," *Mater. Sci. Eng.*, **A107**, 227–39 (1989).

[3]D. Marshall and A. G. Evans, "Failure Mechanisms in Ceramic-Fiber/Ceramic-Matrix Composites," *J. Am. Ceram. Soc.*, **68** [5] 225–31 (1985).

[4]D. B. Marshall, B. N. Cox, and A. G. Evans, "The Mechanics of Matrix Cracking in Brittle Matrix Fiber Composites," *Acta Metall.*, **33** [11] 2013–2021 (1985).

[5]B. Budiansky, J.W. Hutchinson, and A. G. Evans, "Matrix Fracture in Fiber-Reinforced Ceramics," *J. Mech. Phys. Solids*, **34**, 167–89 (1986).

[6]G. C. Sih, Handbook of Stress Intensity Factors. Lehigh University Press, Bethlehem, PA, 1972.

[7]P. G. Charalambides and A. G. Evans, "Debonding Properties of Residually Stressed Brittle Matrix Composites," *J. Am. Ceram. Soc.*, **72** [5] 746–53 (1989).

[8]M.Y. He and J.W. Hutchinson, "A Crack Kinking Out of an Interface," Harvard University Report No. MECH.-113, Harvard University, Cambridge, MA, 1988.

[9]M.Y. He and J.W. Hutchinson, "Crack Deflection at an Interface between Dissimilar Materials," *Int. J. Solids Struct.*, **25** [9] 1053–67 (1989).

[10]A. G. Evans, M.Y. He, and J.W. Hutchinson, "On Interface Debonding and Fiber Cracking in Brittle Matrix Composites"; in The Processing and Mechanical Properties of High Temperature/High Performance Composites. Annual Report, Department of Materials, University of California, Santa Barbara, CA, 1989.

[11]M. D. Thouless, H. C. Cao, and P. A. Mataga, "Delamination from Surface Cracks in Composite Materials," *J. Mater. Sci.*, **24**, 1406–12 (1989).

[12]P. G. Charalambides; unpublished work.

[13]G. Campbell, M. Rühle, B. J. Dalgleish, and A. G. Evans, "Whisker Toughening: A Comparison Between Aluminum Oxide and Silicon Nitride Toughened with Silicon Carbide," *J. Am. Ceram. Soc.*, **73** [3] 521–30 (1990).

[14]M. D. Thouless and A. G. Evans, "Effects of Pull-Out on the Mechanical Properties of Ceramic-Matrix Composites," *Acta Metall.*, **36** [3] 517–22 (1988).

[15]M. D. Thouless, O. Sbaizero, L. S. Sigle, and A. G. Evans, "Effect of Interface Mechanical Properties on Pullout in SiC-Fiber-Reinforced Lithium Aluminum Silicate Glass-Ceramic," *J. Am. Ceram. Soc.*, **72** [4] 525–31 (1989).

[16]B. Cotterell and J. R. Rice, "Slightly Curved or Kinked Cracks," *Int. J. Fract.*, **16**, 155 (1980).

[17]A. G. Evans and J.W. Hutchinson, "Effects of Non-Planarity on the Mixed Mode Fracture Resistance of Bimaterial Interfaces," *Acta Metall.*, **37** [3] 909–16 (1989).

[18]P. G. Charalambides, J. Lund, A. G. Evans, and R. M. McMeeking, "A Test Specimen for Determining the Fracture Resistance of Bimaterial Interfaces," *J. Appl. Mech.*, **56**, 77–82 (1989).

[19]Z. Suo, "Delamination Specimens for Orthotropic Materials"; in The Processing and Mechanical Properties of High Temperature/High Performance Composites. Annual Report, Department of Materials, University of California, Santa Barbara, CA, 1989.

[20]P. G. Charalambides, H. C. Cao, J. Lund, and A. G. Evans, "Development of a Test Method for Measuring the Mixed Mode Fracture Resistance of Bimaterial Interfaces," *Mech. Mater.*, **8**, 269–83 (1990).

[21]M. D. Drory, M. D. Thouless, and A. G. Evans, "On the Decohesion of Thin Films," *Acta Metall.*, **36**, 2019–2028 (1988). □